2022 IEEE 18th International Conference on Automation
Science and Engineering (CASE)
August 20-24, 2022. Mexico City, Mexico

2022 IEEE 18th International Conference on Automation Science and Engineering (CASE) | 978-1-6654-9042-9/22/$31.00 ©2022 IEEE | DOI: 10.1109/CASE49997.2022.9926444

Supervised Adaptive Fuzzy Control of LVAD with Pulsatility Ratio Modulation

Milad Azizkhani[1], Yue Chen[1]

***Abstract*—Left ventricular assistive devices (LVAD) have been used for patients who experience congestive heart failures and are waiting for heart transplantation. These devices can help patients to resume their daily life/work until a suitable donor is found. LVAD mainly consists of a rotary pump that is directly attached from the left ventricle to the aorta using two cannulas. To meet patients' needs, a control algorithm should be implemented to adjust the pump speed in different physiological conditions such as exercising, resting, etc. However, the accurate control of LVADs is still a challenging problem due to the unavailability of hemodynamic variables measurements, the requirement for suction avoidance, and the varying nature of the heart in different scenarios. In this study, a supervised adaptive fuzzy control strategy with pulsatility ratio modulation has been implemented to not only provide enough perfusion for the circulatory system but also to prevent suction phenomena. It has been shown that the proposed adaptive fuzzy control scheme presents a faster response compared to the previously developed fuzzy controller for LVAD and at the same time shows a faster response to push the system out of the suction area if happens. Most importantly, it has been demonstrated that the supervised adaptive fuzzy controller could help the system to stay away from the suction bound compared to the conventional methods.**

***Index Terms*—LVAD, Pulsatility, Supervised Adaptive Fuzzy Control.**

I. Introduction

LEFT ventricular assistive devices (LVADs) are designed to help patients who are experiencing chronic congestive or end-stage heart failures [1], [2]. These devices are utilized to assist the heart in pumping enough blood to the circulation system. LVADs are mostly considered as the temporary but critical treatment for patients who are waiting for heart transplantation since finding a suitable heart donor usually takes a long time, and 20-30 percent of these patients will lose their lives in this process if they don't get access to appropriate treatments such as LVADs [3]. With the technological advancement in the past several decades, continuous flow turbo dynamic pumps (second generation) are vastly used in comparison with the pulsatile pumps since they are lighter, smaller, quieter, more durable, having less surgical trauma, higher energy efficiency, and lower thrombogenicity [4]. The pump will connect the left ventricle to the aorta using two cannulas and create a parallel path for the blood flow.

To meet patients' physiological needs, the speed of these pumps should be adjusted based on patient's condition. A trained clinician can tune the pump speed manually when the patient is monitored. However, staying at hospitals is not a viable option in the long term because the patients need to return to their daily work/life. Thus, it is important to design a controller to adjust the motor speed automatically to satisfy patient needs in different physiological conditions, such as exercising, resting, etc. In addition, the speed adjustment should be performed safely to prevent suction and back-flow in the heart. If the pump works excessively at high speeds, the pump will try to draw more blood than the available amount from the left ventricle, which will result in the collapse of the left ventricle. On the other hand, if the speed of the pump gets lower than the threshold, the blood will come back from the aorta [3], [5].

Considering the above-mentioned requirements, a feedback controller should be designed to address all of the objectives. Different strategies have been used to address the control problem, for instance, heart rate was used to determine the target speed for the pump in [6], while the waveform deformation index was used to adjust the pump speed to prevent the system from the suction area. In another study [7], the control of total artificial heart was addressed by correlating between mixed venous oxygen saturation (Svo2) and cardiac output. Ferreira et al. [8] presented a suction detection algorithm that classifies the system into no suction, moderate suction, and severe suction states based on discriminant analysis. The obtained scores was then used in a fuzzy logic controller to adjust the pump speed.

The utilization of sensors in the body for measuring the hemodynamic variables of the system is not a viable option. However, it is feasible to use sensors out of the body to perform the measurement. Pump flow measurements, which can be obtained using an ultra-sonic transducer either in the inlet or outlet cannula are a suitable option to design the control scheme around it [9]. Choi et. al [10] used the pulsatility index (PI) of the flow, which describes the amplitude of the pump flow, to adjust the speed of the motor by using a fuzzy controller. However, their following work [11] indicated that the flow PI is not a suitable feature to be used as a control index. Based on the system suction state, the increase in pump speed can lead to different flow PI behaviour, which makes the control problem complicated.

This research is funded by Georgia Institute of Technology Faculty Startup Grant, IRIM Seed Grant, and Faculty Relief Grant. Corresponding author: Yue Chen.

[1]Milad Azizkhani and Yue Chen are with the Department of Biomedical Engineering, Georgia Institute of Technology/Emory University, Atlanta, GA, 30332. mazizkhani3@gatech.edu yue.chen@bme.gatech.edu

Additionally, controlling the flow PI won't necessarily satisfy the control objectives such as unloading, perfusion, and safety from the suction. In [11], [12], Choi et al. showed that the pulsatility ratio (PR), which describes the ratio of PI of the pump flow with respect to the head PI of the pump, presents a unique characteristic in which the occurrence of suction can be detected even for patients with weak heart conditions that the flow PI cannot handle. Using a unified index that guarantees enough perfusion for the circulatory system while preventing the system from suction region is an interesting area that needs to be further investigated.

In this paper, we mainly focus on proposing an alternative control approach that can improve the performance of the system, rather than focusing on a new algorithm to estimate or detect the suction phenomena. The left ventricle lumped parameter model of the heart along with the LVAD [9] is used to validate our proposed control scheme. It has been assumed that the right ventricle is healthy or its behavior does not affect the left ventricle model [9]. In this study, the pulsatility ratio is considered as the control index and the control objectives are listed as follows:

1) Improve the tracking performance of the controller in response time and reduce the tracking error.
2) Resolve the tuning issue of fuzzy logic controllers by designing an adaptive fuzzy controller that can adjust its performance based on its objective.
3) Prevent the system from going into the suction area.

The rest of the paper is organized as follows. In section II, the left ventricle model of the healthy heart based on [9] is reviewed to model the hemodynamic behavior of the system. In section III, the LVAD is integrated with the heart model and the governing equations are derived. To investigate the effects of an LVAD on the left ventricle model, a simulation study has been conducted. Section IV highlights the previously developed fuzzy control design along with our proposed supervised adaptive fuzzy algorithm by using pulsatility ratio as the control index in both cases. In section V, simulation studies have been conducted to show the superiority of our approach and its effectiveness in satisfying our predefined objectives. In section VI, the result of our paper is discussed, and future directions of our research have been identified.

II. Cardio Vascular Model

In this section, the model of the left ventricle is developed based on [9]. The system is modeled using electrical components where resistors, inductors, and capacitors are associated with blood flow resistance, the inertial effect of the blood flow, and the compliance of blood vessels, respectively. The ventricular pressure corresponds to voltage, and blood flow is related to current. The effect of the left ventricle is modeled using a time-varying capacitance. The elastance is the reciprocal of compliance or capacitance and describes the contractual state of the left ventricle [9]. The elastance of the heart (E_H) is described as follows

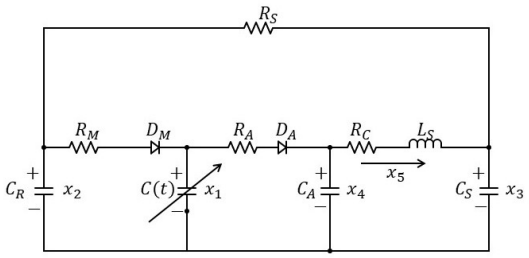

Fig. 1. Lumped parameter model of the left ventricle system [9].

$$
\begin{aligned}
&E_H(t) = (E_{max} - E_{min})E_n(t_n) + E_{min} \\
&E_n(t_n) = 1.55\left(\frac{(t_n/0.7)^{1.9}}{1+(t_n/0.7)^{1.9}}\right)\left(\frac{1}{1+(t_n/1.17)^{21.9}}\right) \\
&t_n = t/T_{max}, \quad T_{max} = 0.2 + 0.15t_c, \quad t_c = 60/HR
\end{aligned} \tag{1}
$$

where E_n denote normalized elastance, t_c cardiac cycle, and HR the heart-rate .

With the introduction of the effect of the left ventricle, the governing dynamic equations of hemodynamic variables of the heart can be derived using a fifth-order lumped parameter model, which is depicted in Fig. 1. The differential equations are derived using Kirchhoff's law, which can be represented in state-space form ($\dot{X} = AX$) as follows

$$
\mathrm{A}=\begin{bmatrix}
-\frac{\dot{C}(t)}{C(t)} - \left(\frac{1}{R_M C(t)} + \frac{1}{R_A C(t)}\right) & \frac{1}{R_M C(t)} & 0 & \frac{1}{R_A C(t)} & 0 \\
\frac{1}{R_M C_R} & -\left(\frac{1}{R_M C_R} + \frac{1}{R_S C_R}\right) & \frac{1}{R_S C_R} & 0 & 0 \\
0 & \frac{1}{R_S C_S} & \frac{-1}{R_S C_S} & 0 & \frac{1}{C_S} \\
\frac{1}{R_A C_A} & 0 & 0 & \frac{-1}{R_A C_A} & \frac{-1}{C_A} \\
0 & 0 & \frac{-1}{L_s} & \frac{1}{L_S} & \frac{-R_C}{L_S}
\end{bmatrix} \tag{2}
$$

where $x_1(t), x_2(t), x_3(t), x_4(t)$, and $x_5(t)$ denotes left ventricle pressure (LVP [mmHg]), left atrial pressure (LAP [mmHg]), arterial pressure (AP [mmHg]), aortic pressure (AoP [mmHg]), and total flow (Q_T [ml/s]) of the heart, respectively. The system described by (2) can model four phases of the heart, namely isovolumic relaxation, filling, ejection, and isovolumic contraction, which are determined by mitral (R_M) and aortic (R_A) valve resistances statue as follows

$$
\mathrm{R}_M = \begin{cases} R_{M\,nominal} & x_2 \geq x_1 \\ \infty & x_2 < x_1, \end{cases} \quad R_A = \begin{cases} R_{A\,nominal} & x_1 \geq x_4 \\ \infty & x_1 < x_4 \end{cases} \tag{3}
$$

where ∞ denotes the valve is closed, otherwise the valve is open.

III. Cardio Vascular - LVAD Model

Now, we detail the model when the LVAD is attached to the heart by two cannulas from the left ventricle to the aorta. Based on [9] and [12], the lump parameter model is depicted in Fig. 2. The characteristics of the cannulas are modeled by a resistor and inductor in series in the path of the pump. The pressure difference across the pump is derived based on the simplified model presented in [13] as

$$
\Delta P = \beta_0 x_6 + \beta_1 \dot{x}_6 + \beta_2 \omega^2 \tag{4}
$$

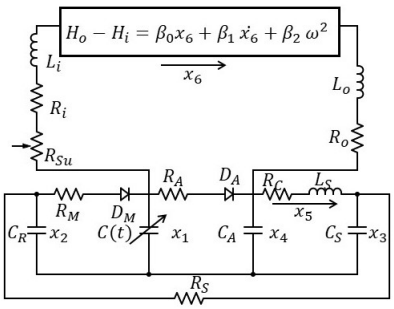

Fig. 2. Left ventricle with LVAD lumped parameter model.

where ω is the pump speed in rpm, x_6 is the pump flow, $\beta_0 = -0.01707, \beta_1 = -0.02177$, and $\beta_2 = 9.9025e^{-7}$. This model allows for the estimation of the pump head without additional sensors. To take into account the suction phenomena, a resistor is implemented into the system [9], [14] and is described as follows

$$R_{su} = \begin{cases} 0 & \text{if} \quad x_1(t) > \overline{x_1} \\ -3.5\,(x_1(t) - \overline{x_1}) & \text{if} \quad x_1(t) \le \overline{x_1} \end{cases} \tag{5}$$

where ($\overline{x_1} = 1$) is the threshold. Now the new path equations can be derived based on Kirchhoff's law as

$$\begin{aligned} x_1 - x_4 &= (R^*)\,x_6 + (L^*)\,\dot{x}_6 - \beta_2\omega^2 \\ R^* &= R_{su} + R_i - \beta_0 + R_0,\, L^* = L_i - \beta_1 + L_0 \end{aligned} \tag{6}$$

where $R_i = R_o = 0.0677$ are inlet and outlet resistance, and $L_i = L_o = 0.0127$ are inlet and outlet inertance [9]. Considering equation (6) in the heart model, state-space equation is derived as ($\dot{X} = A_c X + B_c U$), where A_c is described as follows

$$\begin{aligned} A_c &= \begin{bmatrix} A & A_c(1,2) \\ A_c(2,1) & A_c(2,2) \end{bmatrix} \\ A_c(1,2) &= [-1/C(t), 0, 0, 1/C_A, 0]^T \\ A_C(2,1) &= [1/L^*, 0, 0, -1/L^*, 0]\,, A_c(2,2) = -R^*/L^* \end{aligned} \tag{7}$$

where $U = \omega^2$, and the B_c is described as $B_c = \left[0, 0, 0, 0, 0, \frac{\beta_2}{L^*}\right]^T$. To investigate the suction phenomena, the system is subjected to a linearly increasing input $\omega(t) = 1.2 \times 10^4 + 100t$, and the response of the system is depicted in Fig. 3. As can be seen, the pump flow increases with the increment of the motor pump speed, but a sudden flow drop is observed and the flow envelop diagram changes. This breakpoint is considered as the starting point of the suction phenomena. It has been shown that the location of this breakpoint will change as the activity mode of the patient changes [3].

IV. Controller Design

A. Pulsatility Ratio

In this study, it is assumed that the only available measurement is the pump flow, which can be easily obtained [9]. The PI of an artificial signal is described as follows

$$S(t)_{pul} = G_L(abs(G_H(S(t)))) \tag{8}$$

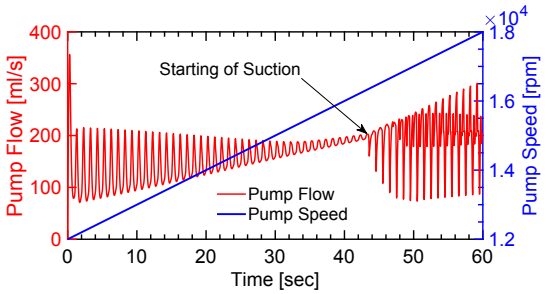

Fig. 3. Forced system simulation subject to a linearly increasing input.

where G_L, and G_H denote low pass and high pass filters respectively. The cutoff frequency of the low pass and high pass filters is chosen to be 0.25 and 0.75 hertz, respectively [11]. The pulsatility ratio (PR) is defined as the ratio between pump flow PI to pump head PI as follows

$$\text{PR} = \frac{Q_{pul}}{\Delta P_{pul}} \tag{9}$$

B. Fuzzy Control for Pulsatility Ratio

Choi et. al used PR instead of flow PI for controlling the LVAD [11]. It has been shown using this feature as a control index can help the system to generate enough perfusion for the body and provide information about the suction state in the system at the same time. Inputs to the fuzzy controller are described as follows:

$$e = \text{PR}_{\text{sys}} - \text{PR}_{\text{ref}}, \quad \Delta e(k) = e(k) - e(k-1) \tag{10}$$

where PR_{sys} is the system PR and PR_{ref} is the reference PR. The membership functions of the fuzzy controller are defined by triangular shapes (Table I), and a Mamdani fuzzy inference engine has been used to generate the fuzzy output. For the defuzzification of the fuzzy output, the center average defuzzifier has been implemented. However, it should be noted that it is a time-consuming tuning procedure to drive the membership function, their shape and bounds to get a satisfactory response.

		Δe				
		LN	N	Z	P	LP
e	LN	LN	LN	N	N	Z
	N	LN	LN	N	Z	P
	Z	N	N	Z	P	P
	P	N	Z	P	P	LP
	LP	Z	P	P	LP	LP

TABLE I
Fuzzy rules for fuzzy controller [11]

C. Supervised Adaptive Fuzzy Control

To further improve the performance of the system, while avoiding a time-consuming procedure for tuning, an adaptive control approach is developed to achieve the desired goal. Due to satisfactory results of the fuzzy controller in [11], we develop our adaptive controller on the basis of fuzzy control. In what follows, the controller derivation based on [15] has been discussed. First, the input of the controller needs to be fuzzified. We have used a non-singleton fuzzifier to define the membership of inputs using a bell shape function as follows

$$\mu_{g_i}(x_i) = \exp(-(x_i - c_g)^2/\sigma_g^2) \tag{11}$$

where μ_g denotes the membership value of the input in the class g, c_g is the center of the membership function, and σ_g works as variance, or the width of the Gaussian membership function. The relationship between the membership function and fuzzy output has been calculated by the multiplication t_{norm}. Similar to the controller in IV-B, the center average defuzzifier has been used to defuzzify the output, which is described as follows

$$y(x) = \frac{\sum_{l=1}^{M} \bar{y}^l \prod_{i=1}^{n} \mu_{g_i}^l (x_i)}{\sum_{l=1}^{M} \left(\prod_{i=1}^{n} \mu_{g_i}^l (x_i)\right)} \tag{12}$$

where $\bar{y}^l$ denotes the location where the resulting value of the fuzzy rule l reaches its maximum, n is the number of inputs (states of the system), and M is the number of relations. Although, different parameters in the fuzzy controller can be reformulated to be used as adaptable parameters; in this study, we have assumed that $\bar{y}^l$ is the adaptable parameter. Using the discussion in [15], the regressor matrix will be defined as follows

$$\xi^l(\boldsymbol{x}) = \frac{\prod_{i=1}^{n} \mu_{g_i}^l (x_i)}{\sum_{l=1}^{M} \left(\prod_{i=1}^{n} \mu_{g_i}^l (x_i)\right)} \tag{13}$$

Using (12), and the idea in (13), the output is defined as follows

$$y(\boldsymbol{x}) = \boldsymbol{\theta}^T \xi(\boldsymbol{x}) \tag{14}$$

where $\boldsymbol{\theta} = [\bar{y}^1, \bar{y}^2, ..., \bar{y}^M]^T$. As discussed earlier, the basis of our design is fuzzy control. Fuzzy control can be categorized in black box controllers, meaning the controller does not rely on any information from the model.

It is assumed that our system is a second-order nonlinear function whose dynamics can be described by an unknown nonlinear function of PR and PR difference (The derivative with respect to time has been assumed to be equivalent to difference). The PR dynamics is described as a second-order system as follows

$$\ddot{x} = f(x, \dot{x}) + bu \tag{15}$$

where x denotes the pulsatility ratio of the system. Based on [15], the following control rule should be designed in a way to make the system track the desired trajectory.

$$u = u_c(\boldsymbol{x}, \boldsymbol{\theta}) + u_s(\boldsymbol{x}) \tag{16}$$

where u_c is the adaptive term and u_s is the supervisory term. If the system dynamics were completely known, the following control rule would have guaranteed the stability and tracking.

$$u^* = \frac{1}{b}\left[-f + \ddot{y}_m + k^T e\right] \tag{17}$$

where y_m denotes the desired trajectory. By implementing the control rule of (16) into (15), and adding and subtracting bu^* from the right side of the resulting equation, the closed-loop equation would be described as follows

$$\ddot{e} = -\boldsymbol{k^T} e + b\left[u^* - u_c(\boldsymbol{x}, \boldsymbol{\theta}) - u_s(\boldsymbol{x})\right] \tag{18}$$

Our adaptive control should be able to estimate the u^*, and since it is assumed that f is an unknown nonlinear function, the adaptive rule should be in the format of a universal approximator. It has been shown that the fuzzy logic system in the form of (12) presents universal approximation ability and can estimate the desired nonlinear control rule [15], [16]. To perform the stability proof, equation (18) is transformed to state-space form as follows

$$\dot{E} = \Lambda E + b_c\left[u^* - u_c(\boldsymbol{x}, \boldsymbol{\theta}) - u_s(\boldsymbol{x})\right] \tag{19}$$

By considering the following Lyapunov function $V_e = \frac{1}{2}E^T P E$, with positive definite matrix P which satisfies the following Lyapunov equation

$$\Lambda^T P + P\Lambda = -Q \tag{20}$$

the time derivative of the Lyapunov function can be calculated as follows

$$\begin{aligned} \dot{V}_e &= -0.5E^T Q E + E^T P b_c\left[u^* - u_c\left(\boldsymbol{x}, \boldsymbol{\theta}\right) - u_s(\boldsymbol{x})\right] \\ \dot{V}_e &\le -0.5E^T Q E + \left|E^T P b_c\right|\left(|u^*| + |u_c|\right) - E^T P b_c u_s \end{aligned} \tag{21}$$

As discussed in [15], a supervisory control is derived to guarantee the system remains in the predefined bound for system stability consideration. In our case, this bound is defined as the suction-free stage. The supervisory control, the adaptive control, and the adaptation rule are described as follows

$$\begin{aligned} &u_s(\boldsymbol{x}) = I^* \operatorname{sgn}\left(E^T P b_c\right)\left(|u_c| + \frac{1}{b_L}\left(f^U + |\ddot{y}_m| + \left|k^T E\right|\right)\right) \\ &u_c(\boldsymbol{x}, \boldsymbol{\theta}) = \boldsymbol{\theta}^T \xi(\boldsymbol{x}), \quad \dot{\boldsymbol{\theta}} = \gamma E^T \boldsymbol{p}_n \xi(\boldsymbol{x}) \end{aligned} \tag{22}$$

where $\boldsymbol{p}_n$ is the last column of P, and $I^* = 1$ if $V_e > \bar{V}$, otherwise the effect of I^* would be terminated. f^U and b_L are chosen such that $|f(\boldsymbol{x})| \le f^U$ and $b_L > 0$.To guarantee the boundness of the adaptable parameters, the projection redesign discussed in [15], [17] was added to the original adaptation rule in (22) as follows

$$\dot{\boldsymbol{\theta}} = \begin{cases} \gamma \mathbf{E}^T \mathbf{p}_n \xi(\mathbf{x}) & \text{if } (|\boldsymbol{\theta}| < M_\theta) \text{ or } (|\boldsymbol{\theta}| = M_\theta \\ & \quad \text{and } \mathbf{E}^T \mathbf{p}_n \boldsymbol{\theta}^T \xi(\boldsymbol{x})) \le 0) \\ \gamma \mathbf{E}^T \mathbf{p}_n \xi(\mathbf{x}) - \gamma \mathbf{E}^T \mathbf{p}_n \frac{\boldsymbol{\theta}\boldsymbol{\theta}^T \xi(\mathbf{x})}{|\boldsymbol{\theta}|^2} & \text{if } (|\boldsymbol{\theta}| = M_\theta \text{ and } \mathbf{E}^T \mathbf{p}_n \boldsymbol{\theta}^T \xi(\mathbf{x}) > 0), \end{cases} \tag{23}$$

where γ represent adaptation gain and will be chosen as a constant value.

V. Simulation Study

A. Fuzzy vs Adaptive Fuzzy Control

In this simulation study, different physiological needs of patients have been considered by changing the systemic vascular resistance (SVR), R_S value. The decrease in R_S indicates an increase in the activity level of the patient [3]. During the simulation, it is assumed that the patient is in the lowest level of activity at first, for instance being asleep, and then changing to higher-level activities abruptly in three steps. In reality, the SVR would not change with this rate; however, to highlight the ability of our controller, the abrupt change in the SVR, due to different physiological conditions, has been considered. The simulation was conducted for a period of 130 s for a very sick heart $E_{max} = 0.6, E_{min} = 0.06$, and Heart Rate = 60 bpm. The SVR value is initially $R_S = 2$, and changed to 1.5, 1, and 0.5 at 50, 80, 100 s, respectively. The reference PR is considered to be 0.51. It

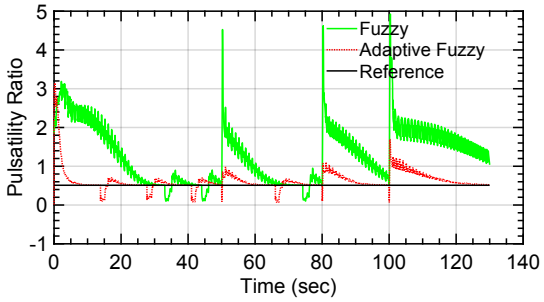

Fig. 4. Tracking performance comparison of the fuzzy and the adaptive fuzzy controller.

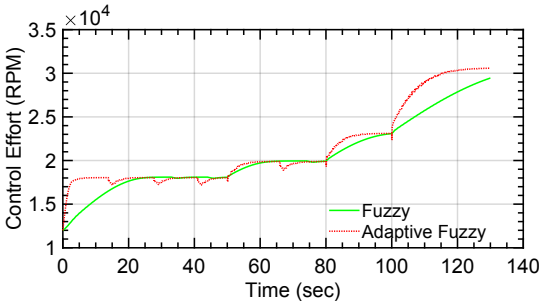

Fig. 5. Control effort comparison of the fuzzy and the adaptive fuzzy controller.

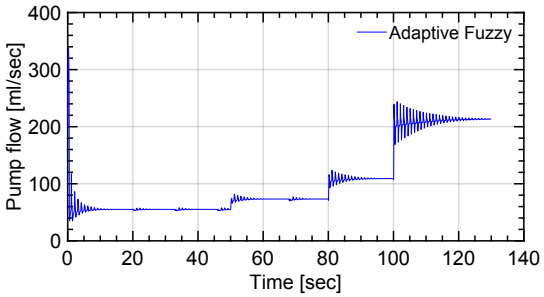

Fig. 6. Pump flow response of the system subject to the adaptive fuzzy controller.

has been shown that this PR can provide maximum perfusion to the heart [11]. As can be seen in Fig. 4, both fuzzy and adaptive fuzzy control (without supervisory term) were able to reach the desired PR. To adjust the control parameters, first Λ was defined as $[[0,1]^T,[-100,-10]^T]^T$ and $Q = diag([1,1])$ to define the closed-loop system behavior. To provide a fair comparison, similar to controller explained in IV-B, five membership functions have been considered for each input. However, the shape and the bound of each controller is tuned individually due to different mechanism of each control scheme. Triangular membership function for controller in IV-B presented a slightly better performance with respect to bell shape membership functions. The membership functions for adaptive fuzzy control scheme are designed based on (22) due to global approximation behaviour of Gaussian functions. The center of membership functions of PR and PR difference for adaptive fuzzy control scheme are considered in the bound of [-0.3,0.3] and [-1,1] with equal steps, respectively. The adaptation gain and the bound of the L_2 norm of the adaptable parameters are chosen as $\gamma = 5 \times 10^6$ and $M_\theta = 5 \times 10^5$, respectively. To prevent the back-flow at the start of the simulation, the pump speed offset has been set to 12000 rpm.

Both controllers were able to force the system track the desired PR, which is depicted in Fig. 4. As expected, the pump speed has been increased to meet the physiological need of the patient. The adaptive fuzzy controller presented a faster response in comparison to the fuzzy controller, which highlights the superiority of this proposed approach. The fast response can be further highlighted in Fig. 5, where the control outputs are compared with each other. The PR drop after reaching the desired ratio in Fig. 4 indicates the occurrence of suction in the system, and as expected both controllers decreased their speed to push the system out of the suction area. The flow of the pump for the adaptive fuzzy control case is also shown in Fig. 6. As can be seen, the flow has increased to provide enough perfusion for the patient at different scenarios.

B. Supervised Adaptive Fuzzy Control

As discussed earlier, preventing the system from entering the suction area is of great importance. This problem is circumvented by defining a safe boundary output and observing the Lyapunov function value bound. A supervisory term has been added to the adaptive control term to push the system to the safe region when the system approaches the suction area. The control parameters of supervisory term are chosen as $\bar{V} = 0.03$, $f^U = 10$, $b_L = 100$, and the number of membership function for each input has increased to seven with the same bounds. As can be seen in Fig. 7, although the system has not reached the exact value of the reference pulsatility ratio, it maintained its bound in that vicinity. In this way, the system has lost some minor perfusion, but it maintained the system in the suction-free region. One of the disadvantages of this control design can be associated with the high activity of the controller which is depicted in Fig. 8. This result indicates the need for better control rules to satisfy the suction-free area without high control activity. To highlight the performance of the supervised adaptive fuzzy controller, the flow of the pump is depicted in Fig. 9.

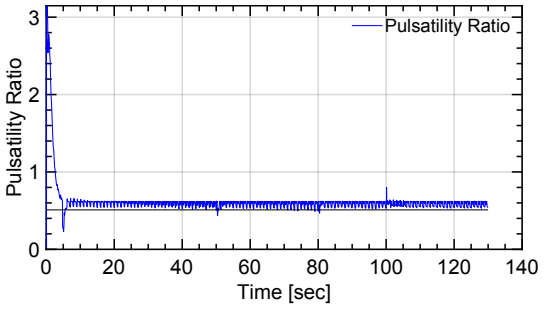

Fig. 7. The tracking performance of the supervised adaptive fuzzy controller.

VI. Discussion and Conclusion

In this study, adaptive fuzzy control and supervised adaptive fuzzy control of an LVAD have been proposed to satisfy three challenges in the feedback control. First, the structure

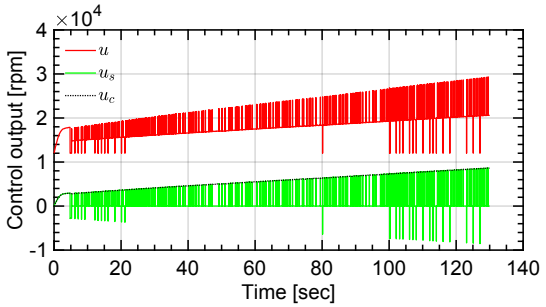

Fig. 8. Control effort of the supervised adaptive fuzzy controller. The supervised, adaptive, and total effort are shown in green, dashed-black, and red, respectively.

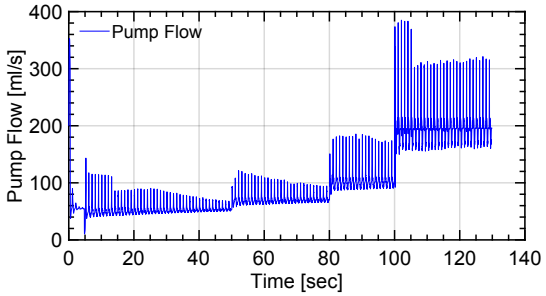

Fig. 9. Pump flow response of the system subject to the supervised adaptive fuzzy control scheme.

of the adaptive control scheme makes the design and tuning of the controller more efficient. In the fuzzy control, the expert needs to modify the rules and membership functions to get a satisfactory response. In comparison, the tunable parameters in the adaptive control scheme are the bounds of inputs and adaptation gains, which makes the tuning process straightforward. The adaptation algorithm helps the system to improve itself online using its objective of reaching the desired pulsatility ratio. The second improvement in the adaptive fuzzy control is increasing the convergence speed of the controller. The third advantage, which comes from adding the supervised term to the adaptive fuzzy controller, is maintaining the system out of the suction area. Although the controller shows a fast activity in the control output, it prevents the system from entering the suction region. This behavior proves the concept that the system can be out of the suction area, however, the supervised term must be modified to get a satisfactory response in the control output.

In our future studies, we plan to address the supervised term high control activity by merging the benefits of data-driven and model-based approaches. Since the proposed approach in this article completely relies on the measured data from pump flow and indirect calculation of pulsatility ratio, the supervised term is activated when the system reaches a predefined error bound, which needs to be tuned by trial and error. Instead, the model information can be used to modify the supervised control algorithm to reduce the supervised control high activity. For instance, by considering the online estimation of SVR [18] and pump speed safe bound in different physiological conditions [3], the supervised term can be activated using a multi-objective optimal control design, which potentially will reduce the high control activity.

Acknowledgment

The authors would like to thank Mishek Musa for proof-reading the final manuscript.

References

[1] N. C. Dang, V. K. Topkara, B. T. Kim, M. L. Mercando, J. Kay, and Y. Naka, "Clinical outcomes in patients with chronic congestive heart failure who undergo left ventricular assist device implantation," *The Journal of thoracic and cardiovascular surgery*, vol. 130, no. 5, pp. 1302–1309, 2005.

[2] E. A. Rose, A. C. Gelijns, A. J. Moskowitz, D. F. Heitjan, L. W. Stevenson, W. Dembitsky, J. W. Long, D. D. Ascheim, A. R. Tierney, R. G. Levitan, *et al.*, "Long-term use of a left ventricular assist device for end-stage heart failure," *New England Journal of Medicine*, vol. 345, no. 20, pp. 1435–1443, 2001.

[3] M. A. Simaan, A. Ferreira, S. Chen, J. F. Antaki, and D. G. Galati, "A dynamical state space representation and performance analysis of a feedback-controlled rotary left ventricular assist device," *IEEE Transactions on Control Systems Technology*, vol. 17, no. 1, pp. 15–28, 2008.

[4] D. Barić, "Why pulsatility still matters: a review of current knowledge," *Croatian medical journal*, vol. 55, no. 6, pp. 609–620, 2014.

[5] J. Martina, N. Jonge, M. Rutten, J. H. Kirkels, C. Klöpping, B. Rodermans, E. Sukkel, N. Hulstein, B. Mol, and J. Lahpor, "Exercise hemodynamics during extended continuous flow left ventricular assist device support: the response of systemic cardiovascular parameters and pump performance," *Artificial Organs*, vol. 37, no. 9, pp. 754–762, 2013.

[6] K. Ohuchi, D. Kikugawa, K. Takahashi, M. Uemura, M. Nakamura, T. Murakami, T. Sakamoto, and S. Takatani, "Control strategy for rotary blood pumps," *Artificial organs*, vol. 25, no. 5, pp. 366–370, 2001.

[7] M. Nakamura, T. Masuzawa, E. Tatsumi, Y. Taenaka, T. Nakamura, B. Zhang, T. Nakatani, H. Takano, and T. Ohno, "The development of a control method for a total artificial heart using mixed venous oxygen saturation," *Artificial Organs*, vol. 23, no. 3, pp. 235–241, 1999.

[8] A. Ferreira, J. R. Boston, and J. F. Antaki, "A control system for rotary blood pumps based on suction detection," *IEEE Transactions on Biomedical Engineering*, vol. 56, no. 3, pp. 656–665, 2008.

[9] M. A. Simaan, *Rotary Heart Assist Devices*, pp. 1409–1422. Berlin, Heidelberg: Springer Berlin Heidelberg, 2009.

[10] S. Choi, J. Antaki, R. Boston, and D. Thomas, "A sensorless approach to control of a turbodynamic left ventricular assist system," *IEEE Transactions on Control Systems Technology*, vol. 9, no. 3, pp. 473–482, 2001.

[11] S. Choi, J. R. Boston, and J. F. Antaki, "Hemodynamic controller for left ventricular assist device based on pulsatility ratio," *Artificial organs*, vol. 31, no. 2, pp. 114–125, 2007.

[12] S. Choi, J. R. Boston, and J. F. Antaki, "An investigation of the pump operating characteristics as a novel control index for lvad control," *International Journal of Control, Automation, and Systems*, vol. 3, no. 1, pp. 100–108, 2005.

[13] S. Choi, J. Boston, D. Thomas, and J. F. Antaki, "Modeling and identification of an axial flow blood pump," in *Proceedings of the 1997 American Control Conference (Cat. No. 97CH36041)*, vol. 6, pp. 3714–3715, IEEE, 1997.

[14] H. Schima, J. Honigschnabel, W. Trubel, and H. Thoma, "Computer simulation of the circulatory system during support with a rotary blood pump.," *ASAIO transactions*, vol. 36, no. 3, pp. M252–4, 1990.

[15] L.-X. Wang, "Stable adaptive fuzzy control of nonlinear systems," *IEEE Transactions on fuzzy systems*, vol. 1, no. 2, pp. 146–155, 1993.

[16] L.-X. Wang, J. M. Mendel, *et al.*, "Fuzzy basis functions, universal approximation, and orthogonal least-squares learning," *IEEE transactions on Neural Networks*, vol. 3, no. 5, pp. 807–814, 1992.

[17] G. C. Goodwin and D. Q. Mayne, "A parameter estimation perspective of continuous time model reference adaptive control," *Automatica*, vol. 23, no. 1, pp. 57–70, 1987.

[18] E. S. Rapp, S. R. Pawar, J. R. Gohean, E. R. Larson, R. W. Smalling, and R. G. Longoria, "Estimation of systemic vascular resistance using built-in sensing from an implanted left ventricular assist device," *Journal of Engineering and Science in Medical Diagnostics and Therapy*, vol. 2, no. 4, p. 041008, 2019.